ARTICLE IN PRESS

YEXNR-09832; No. of pages: 13; 4C:

Experimental Neurology xxx (2008) xxx-xxx

Contents lists available at ScienceDirect

Experimental Neurology

journal homepage: www.elsevier.com/locate/yexnr

Central adaptation following heterotopic hand replantation probed by fMRI and effective connectivity analysis

S.B. Eickhoff [a,*], M. Dafotakis [a], C. Grefkes [b], N.J. Shah [a,c], K. Zilles [a,c,d], H. Piza-Katzer [e]

[a] Institut für Neurowissenschaften und Biophysik – Medizin (INB 3), Forschungszentrum Jülich, Germany
[b] Max-Planck-Institute for Neurological Research, University of Cologne, Germany
[c] Brain Imaging Center West (BICW), Juelich, Germany
[d] C. & O. Vogt Institute for Brain Research, Heinrich-Heine-University Düsseldorf, Germany
[e] Department of Plastic Surgery, Medical University Innsbruck, Austria

ARTICLE INFO

Article history:
Received 14 January 2008
Revised 29 February 2008
Accepted 17 March 2008
Available online xxxx

Keywords:
M1
SMA
PMC
Plasticity
Connectivity
Replantation
Motor cortex
Network

ABSTRACT

In this functional magnetic resonance imaging (fMRI) study, we examined changes – relative to healthy controls – in the cortical activation and connectivity patterns of two patients who had undergone unilateral heterotopic hand replantation. The study involved the patients and a group of control subjects performing visually paced hand movements with their left, right, or both hands. Changes of effective connectivity among a bilateral network of core motor regions comprising M1, lateral premotor cortex (PMC), and the supplementary motor area (SMA) were assessed using dynamic causal modelling. Both patients showed inhibition of ipsilateral PMC and SMA when moving the healthy hand, potentially indicating a suppression of inference with physiological motor execution by the hemisphere controlling the replanted hand. Moving the replanted hand, both patients showed increased activation of contralateral PMC, most likely reflecting the increased effort involved, and a pathological inhibition of the ipsilateral on the active contralateral M1 indicative of an unsuccessful modulation of the inhibitory M1–M1 balance. In one patient, M1 contralateral to the replanted hand experienced increased tonic (intrinsic connectivity) and phasic (replanted hand movement) facilitating input, whereas in the other, pathological suppression was present. These differences in effective connectivity correlated with decreased behavioural performance of the latter as assessed by kinematic analysis, and seemed to be related to earlier and more intense rehabilitative exercise commenced by the former. This study hence demonstrates the potential of functional neuroimaging to monitor plastic changes of cortical connectivity due to peripheral damage and recovery in individual patients, which may prove to be a valuable tool in understanding, evaluating and enhancing motor rehabilitation.

Introduction

The control of voluntary movements relies on a network of cortical and subcortical brain regions interacting through excitatory or inhibitory circuits to produce the final output to spinal motor neurons (Gerloff and Andres, 2002; Grefkes et al., 2007; Halsband and Lange, 2006; Rizzolatti and Luppino, 2001). Disruption of the dynamic interplay within this network by injury or pathology, however, may prevent normal motor function and force the central nervous system to adapt by re-organising the existing network architecture. These changes are made possible by the brain's capacities for both functional (modifying computational substrates or mechanisms) and structural (axonal rewiring) plasticity as demonstrated in various animal models (Ding et al., 2005; Nudo et al., 1996, 2003; Pizzi et al., 2006; Schallert et al., 2000, 2003).

Probably the most important mechanism for disturbances of cortical networks is the damage and hence incapacitation of participating areas or pathways by, e.g., trauma or stroke. Studies which investigated the plastic changes in the human brain due to such (central) injuries often observed a shift in the functional architecture, with neighboring or homologous areas filling in for the damaged regions (Chollet and Weiller, 1994; Weiller et al., 1992). Important examples for this adaptation include the remapping of somatotopic cortex following circumscribed lesions affecting the corticospinal tract (Ward and Cohen, 2004) or the increased recruitment of the right inferior frontal gyrus in language tasks due to ischemia in Broca's region (Lindberg et al., 2007; Saur et al., 2006; Schaechter et al., 2006). Contrasting our knowledge on the effects of central lesions, less attention has been devoted to the adaptive plasticity of cortical networks following peripheral pathology such as nerve injuries and affections to the respective receptor (sensory epithelium) or effector (muscles) organs. However, the observation of widespread cortical re-organisation in non-congenitally

* Corresponding author. Institute of Neurosciences and Biophysics – Medicine (INB-3), Forschungszentrum Jülich GmbH, Leo-Brandt Street 5, 52425 Jülich, Germany. Fax: +49 2461 61 2820.
E-mail address: S.Eickhoff@fz-juelich.de (S.B. Eickhoff).

0014-4886/$ – see front matter © 2008 Elsevier Inc. All rights reserved.
doi:10.1016/j.expneurol.2008.03.025

blind subjects (Burton et al., 2002, 2004; Goyal et al., 2006) raises the question about the nature of adaptive changes in cortical motor control following manipulation to its peripheral effectors. In other words, can plastic adaptation of motor networks be observed following changes in the anatomy of joints, muscles and nerves as previously hypothesised for tool use (Johnson-Frey, 2003; Maravita and Iriki, 2004)? Furthermore, do these changes reflect the degree of proficiency in the voluntary use of this non-physiological anatomy?

To address these questions, we investigated two patients following heterotopic hand replantation. Both underwent surgery for malignant soft tissue tumours of the proximal forearm with extensive resection of the affected tissue and subsequent heterotopic re-implantation of the amputated distal forearm (incl. the hand) to the stump of the upper arm (Piza-Katzer et al., 2006; Windhager et al., 1995). Tendons of the finger flexors and extensors were attached to the proximal arm muscles which now initiate finger movements causing a radical change of the peripheral motor effectors. Over time, both patients managed to adapt their motor skills and have regained behaviourally relevant capacities for voluntary hand movements (Piza-Katzer et al., 2006; Windhager et al., 1995).

In the current study, regained hand function and continuing disturbances in motor execution were assessed in these patients by kinematic motion analysis, while changes in cortical activation were revealed by functional magnetic resonance imaging (fMRI). Furthermore, dynamic causal modelling (DCM) was used to demonstrate changes in cortical connectivity representing the central adaptation processes following peripheral hand replantation.

Materials and methods

Patients

Both patients investigated in this study (Fig. 1) were diagnosed with malignant soft tissue tumours of the forearm whose radical resection necessitated removal of the elbow joint. However, as neither of the patients consented to upper arm amputation, the procedure generally recommended in such cases, both underwent heterotopic replantation of the amputated distal third of the forearm together with the hand to the stump of the upper arm. The surgical procedure, which has already been described in detail (Piza-Katzer et al., 2006; Windhager et al., 1995) involved the attachment of the tendineous structures of the forearm to the three muscles of the upper arm, and a coaptation of the nerves of the distal forearm with the nerve trunks of the upper arm.

Patient GM is a 42 year old formerly right-handed male, who was operated on 18 years ago for recurrent synovial sarcoma of the right forearm. Postoperatively, this patient developed an extended haematoma, necessitating surgical revision with split-thickness skin graft to cover the defect on the forearm. Long-time immobilisation together with a conservative approach to mobility had resulted in a primary use of the formed dominant right hand for auxiliary grip and hold functions and a complete re-training of all fine motor skills to the healthy left hand.

Patient JH is a 29 year old right-handed male, who was operated on 2 years ago for a multi-centric epitheloidsarcoma of the left forearm/elbow. As in his case, surgery yielded a very good initial result, passive and active mobilisation exercise could be commenced from the 3rd post-operative day and was performed for increasing time-spans over 2–3 sessions per day. These exercises resulted in a restoration of (virtually forceless) grip function 10 days after surgery. Following the training of proprioceptive and somatosensory discrimination as well as electrical stimulation of the internal hand muscles (which was continued up to six months after surgery), the patient was able to start re-learning the use of everyday tools using his replanted hand after 4 weeks and resistance training was added another 3 weeks later. This rehabilitative exercise resulted in a good recovery of hand function, which now allows the patient to fully use his replanted left hand in everyday life up to the point where he – by self report – "forgets that the elbow has been removed".

Control subjects

14 subjects (8 males) with no history of neurological or psychiatric diseases served as a healthy control population. All participants gave informed consent before participating in the experiment and had a right hand preference as determined by the Edinburgh handedness questionnaire (Oldfield, 1971). The mean age of the subjects was 36+/−12 years.

Kinematic motion analysis

We used a reach-to-grasp movement paradigm representing an integral part of our daily motor repertoire to assess the motor performance of the patients' healthy and replanted hands. The movement kinematics were recorded using an ultrasonic motion analyser as described elsewhere in detail (Nowak et al., 2007). The task was to grasp an instrumented cylindrical object. Patients placed their hand with thumb and index finger touching each other on a starting mark. Subjects reached for the cylindrical object (diameter: 9 cm, width: 4 cm, weight: 350 g), grasped it between the tips of the index finger and thumb, lifted it 10 cm above the table (as indicated by another mark), held it for 3 s before placing it back on the table. 12 such reach-to-grasp movements were performed by each subject with each hand, the first 4 of which were discarded from further analysis to allow the subjects to get familiar with the task. The patients were instructed to perform the movements quickly but accurately. Movement markers

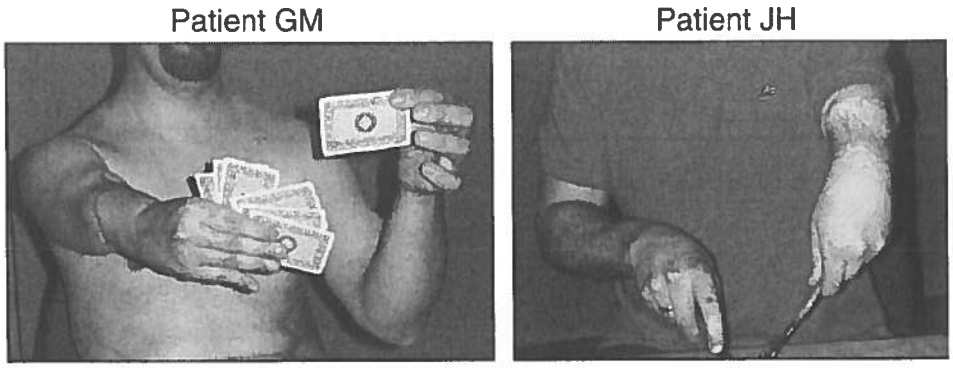

Fig. 1. These recent photographs of the two patients depict their use of the heterotopic hand replants (right hand in the case of GM, left hand for JH) during normal daily activities.

Please cite this article as: Eickhoff, S.B., et al., Central adaptation following heterotopic hand replantation probed by fMRI and effective connectivity analysis, Exp. Neurol. (2008), doi:10.1016/j.expneurol.2008.03.025

on the index finger, thumb and styloid processus of the radius were used to record the spatial and temporal movement characteristics for latter off-line analysis. For each reach-to-grasp movement, the following parameters were obtained: (i) peak of vertical wrist position (in mm), (ii) movement time (in ms), (iii) peak of vertical wrist velocity (in mm/s), (iv) peak grasp aperture (in mm), and (v) peak velocity of grasp aperture (in mm/s). The reach-to-grasp movement required accurate coordination between both proximal and distal arm segments, and is therefore well-suited to investigate sensorimotor integration (Nowak et al., 2007). We calculated the time point of peak grasp aperture in percentage of movement time, which emerges in healthy people between 60 and 80% of the total hand transport component, and represents the cerebral mechanisms of temporo-spatial coupling (Nowak et al., 2007). All parameters were averaged across all trials performed by each of the two participants.

fMRI experimental setup

Subjects were asked to perform simple whole hand fist closing movements with the left hand, the right hand or both hands simultaneously (in-phase) in a bock-design after familiarization to the task outside of the scanner. The instruction for the upcoming block was presented to the participants lying inside the scanner on a custom-built, shielded TFT screen at the rear end of the scanner visible via a mirror mounted on the headcoil (14°×8° horizontal×vertical viewing angle, 245 mm distance from the subject's eyes). As both patients and all controls reported normal uncorrected vision on both eyes, normal binocular perception of the stimuli was possible throughout the experiment. After a jittered delay of 1.5–2.5 s, the circle started blinking red, and the patients performed the fist closing movements synchronously to these blinks. The frequency of the circle cueing the patients was individually determined according to the motor abilities of the patients, i.e., patients could perform the task without signs of fatigue or other constraints (1 Hz for patient JH, 0.8 Hz for patient GM). Control subjects ($n=14$) were paced with 1.5 Hz as described elsewhere (Grefkes et al., 2007) After 15 s, the blinking circle was replaced by a white screen indicating the subjects to rest until the next instruction. The duration of the resting baseline lasted between 11 and 13.5 s depended on a delay between the instruction and the start of the cue, resulting in a fixed block onset asynchrony of 30 s. The experiment consisted of 24 activation blocks and 26 resting baselines (baselines at the beginning and end of the fMRI time-series). The order of conditions was pseudo-randomized and counterbalanced across subjects. Within the scanner, the subject's hands were placed in a neutral position between supination and pronation next to the hips. During the experiment, the performance was monitored by video camera for later off-line analysis.

Image acquisition and processing

Functional MR images were acquired on a Siemens Trio 3.0 T whole-body scanner using a blood oxygenation level dependent (BOLD) gradient echo EPI sequence [TR: 1600 ms, TE: 30 ms, FA: 90°, 26 axial slices (3.0 mm thickness, 0.3 mm gap), in-plane resolution: 3.1×3.1 mm]. Images covered the brain extending from mid-prefrontal to parietal and visual cortex. The cerebellum, orbitofrontal cortex and anterior temporal cortex were outside the limited field of view, necessary to allow for a short TR and hence a reliable estimation of coupling parameters (Friston et al., 2003). Each fMRI time-series consisted of 457 images preceded by 4 dummy scans allowing the MR scanner to reach a steady T2* contrast.

For image preprocessing, statistical analysis and dynamic causal modelling, we used the SPM 5 software package (http://www.fil.ion.ucl.ac.uk). After discarding the dummy images and realignment of the EPI volumes (Ashburner and Friston, 2003), a mean EPI image was computed and spatially normalised using the unified segmentation approach (Ashburner and Friston, 2005) to the standard space of the Montreal Neurological Institute (MNI space). An isotropic 8 mm Gaussian smoothing kernel was applied in order to attenuate noise and residual differences in functional anatomy after normalisation. For statistical analysis by means of a general linear model, box-car reference functions for each condition were convolved with a canonical hemodynamic response (Kiebel and Holmes, 2003). In order to exclude movement-related variance from the time-series, the motion parameter describing the position of each scan relative to the first image of the series were added as covariates into the GLM. These parameters were derived from realignment algorithm as employed during preprocessing and consist of six values per scan (x-translation, y-translation, z-translation, yaw-, pitch-, roll-plane). Together, they cover the full range of rigid-body movements possible in 3D space and should correct for any signal variation ascribable to between-scan head movement.

The resulting parameter estimates were subsequently processed in a second-level analysis of variance (ANOVA including appropriate non-sphericity correction) with the factor "hand" (left/right/both) and "group" (controls, JH, GM — note that each patient formed an individual

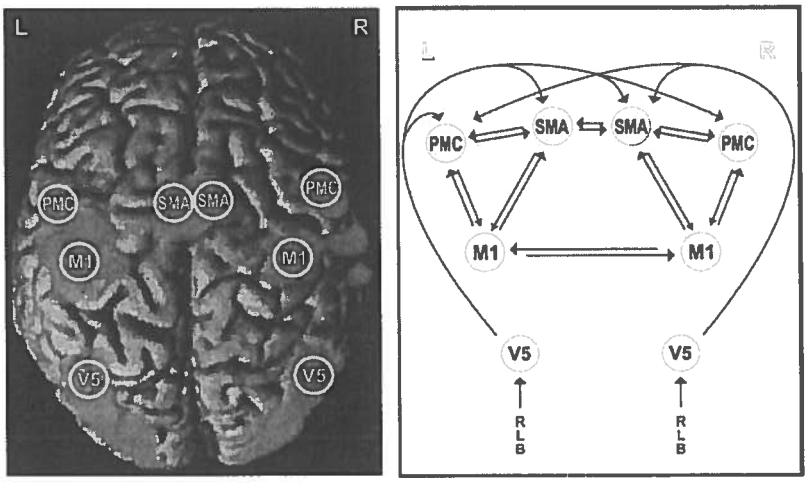

Fig. 2. The left panel shows the location of the ROIs overlaid on the effects of interest map (thresholded at $p<0.05$, FWE corrected) rendered on the MNI single subject template. The right panel shows the architecture of the cortical motor network as assessed by the current study. Please note that for each of the connections denoted by the arrows, we estimated the intrinsic connectivity as well as the task-dependent changes thereof during the performance of the three experimental tasks [right hand movement (R), left hand movement (L), bilateral hand movement (B)].

Please cite this article as: Eickhoff, S.B., et al., Central adaptation following heterotopic hand replantation probed by fMRI and effective connectivity analysis, Exp. Neurol. (2008), doi:10.1016/j.expneurol.2008.03.025

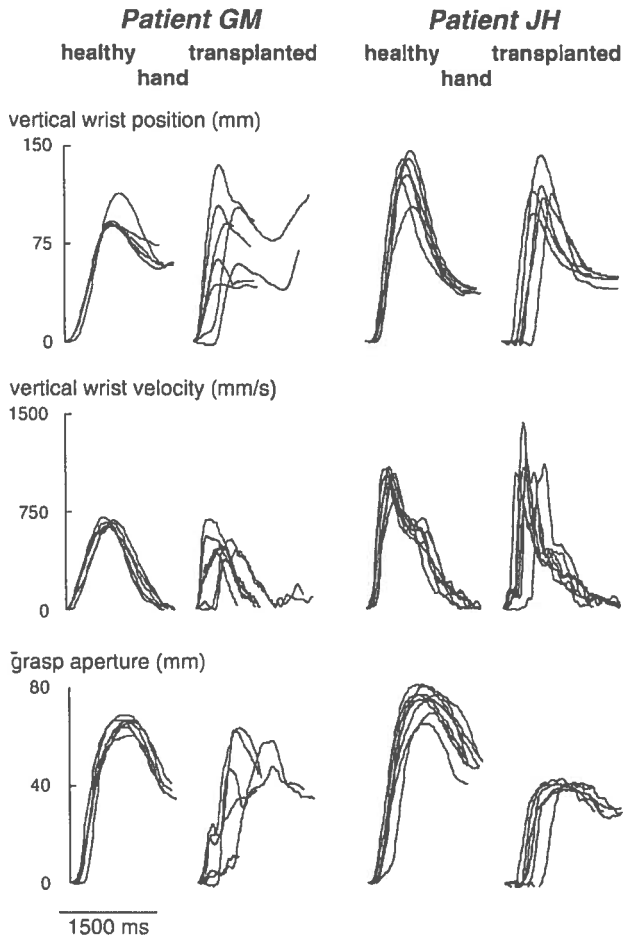

Fig. 3. Kinematic analysis of the patients' performance in the reach-to-grasp task: vertical wrist position in the z-axis and grasp aperture revealed irregular pathways with the replanted hand in both patients. These disturbances, however, were more accentuated in GM. Between them, the patients also showed behavioural differences in vertical wrist velocity patterns when using the replanted hand; GM produced slower and irregular velocity profiles while JH had a more regular pattern with superimposed faster, i.e., ballistic, components indicated by several high peaks. Note that in both patients the behavioural pattern of the healthy hand is within normal range (Nowak et al., 2007).

group and were not averaged due to the difference in affected hand), in a random effects model. Activated regions and differences in brain activity between patients and controls were identified by means of linear contrasts. For the group analysis, the level of significance was $p<0.05$, family wise error (FWE) corrected for multiple comparisons. To gain sensitivity in the single subject comparisons, the threshold was lowered to $p<0.001$ (unc.) with an extended threshold of $k=20$ voxels (Friston et al., 1999b,a).

Dynamic causal modelling

We used dynamic causal modelling (Friston et al., 2003) to assess effective connectivity between the following regions, which were functionally and anatomically (Eickhoff et al., 2005, 2007b) identified in both hemispheres of each subject: the primary motor cortex (M1 (Geyer et al., 1996)), the supplementary motor area (SMA (Geyer, 2003)), the ventral premotor cortex (PMC (Geyer, 2003)), and extrastriate visual cortex (V5 (Malikovic et al., 2007; Wilms et al., 2005)). The time-series of all ROIs were extracted in a sphere region of interest (radius=4 mm) from the "effects of interest" *F*-contrast ($p<0.001$, uncorrected), and adjusted for effects of interest (mean-correcting the data and removing effects due to head movement). V5, which in contrast with early retinotopic cortex (Amunts et al., 2000; Rottschy et al., 2007), showed a well-defined local maximum in neural activity across all subjects, was defined as the input region because subjects used the visual pacing cue as signal for moving the respective hand. That is, in the present model, we assumed that the driving influence of the visual pacing entered PMC and SMA via the visual cortex. It has to be pointed out, though, that the estimated coupling represents the net effective influence of the cue-evoked activity in visual cortex on frontal motor areas, which must not be misinterpreted as direct anatomical connections between them (Friston et al., 2003). Rather, the estimated coupling rates implicitly capture the influence of putative subcortical relay structures, such as the basal ganglia or the cerebellum (Halsband and Lange, 2006; Lindberg et al., 2007; Taniwaki et al., 2006).

The network-model which was assessed in the two patients and subsequently compared to our group of healthy control subjects is described in Fig. 2. In this model each of the arrows is associated with three coupling parameters, the intrinsic, task-independent connectivity (cf. below) as well as the task-dependent modulations thereof caused by the three experimental conditions (left hand movement, right hand movement, bilateral hand movement). For the computation of inter-regional interactions within this network, DCM uses a bilinear model (Friston et al., 2003), where the changes in neuronal states over time are modelled according to the following differential equation:

$$\frac{dx}{dt} = \left(A + \sum_{j=1}^{m} u_j B^{(j)}\right) x + Cu.$$

Here, x represents the neuronal state vector of all regions $[x_1, x_2, x_3, \ldots, x_n]^T$, A represents the intrinsic connectivity, $B^{(j)}$ represents the task-dependent modulations in effective connectivity in relation to the input functions u_j, while C represents the influence of direct inputs to the system, again in relation to the input functions u_j. Note that in the present study, each of the 3 input functions $[u_1, u_2, u_3]$ consists only of 0's and 1's denoting the absence or presence of the respective condition j (left, right, bilateral hand movement) in the performed block-design experiment).

It should be mentioned here that in the absence of input, i.e., at time points where all input functions u are 0 (resting baseline), the model reduces to $dx/dt=Ax$, that is, the only connectivity present in the baseline periods between the activation blocks is that which is embodied in the intrinsic connectivity matrix A. If u is unequal zero, however, the intrinsic connectivity is still present in the same manner as during baseline, while the effects of context-dependent changes in coupling ($\Sigma\, u_j B^{(j)} x$) and those of the direct inputs (Cu) add linearly to the former to form the full bilinear equation. In other words, the intrinsic connectivity represents the constant part of the inter-

Table 1

	Hand	Peak lift position (mm)	Movement time (mm/s)	Peak wrist velocity (mm/s)	Peak grasp aperture (mm)	Peak velocity of grasp aperture (mm/s)	Time peak of grasp aperture (percent of movement time)
GM	Healthy	71±15	946±132	1009±622	66±3	326±40	61±7
	Replanted	144±39	1445±311	636±129	46±14	208±95	74±48
JH	Healthy	168±28	1058±103	966±167	75±5	321±49	58±7
	Replanted	157±19	1290±213	1082±211	41±3	269±36	56±8

Peak lift position, movement time and peak wrist velocity represent the hand transport component as peak grasp aperture and peak velocity of grasp aperture represent the distal muscle component of the reach-to grasp task. Note that time peak of grasp aperture as an indicator of temporo-spatial coupling is more affected in the replanted hand of GM as compared to that of JH or either healthy hand (normal range 50–70%, Nowak et al., 2007). All values represent means±standard deviations.

Please cite this article as: Eickhoff, S.B., et al., Central adaptation following heterotopic hand replantation probed by fMRI and effective connectivity analysis, Exp. Neurol. (2008), doi:10.1016/j.expneurol.2008.03.025

regional coupling which is present during task blocks and baseline, while the task-dependent modulations reflect the (additive) change in coupling that can be observed during the performance of a given task.

This neuronal model of effective connectivity is then combined with a hemodynamic forward model to yield BOLD time-series. The optimal model parameters, given the actual measured time-series, are then estimated for the entire model (Fig. 2) by Bayesian inversion using tight, biologically determined priors on the hemodynamic and conservative shrinkage priors on the neuronal parameters.

The significance of the estimated coupling parameters (intrinsic connections and the task-dependent modulations thereof) in controls was first tested by a one-sample two-sided *t*-test. Differences in inter-regional coupling (i.e., connectivity) between JH or GM and our group of control subjects were assessed for each patient individually by means of a two-sample two-sided *t*-test (all analyses $p<0.05$, Bonferroni-corrected for multiple comparisons).

Results

Behavioural performance in reach-to-grasp movements

Fig. 3 illustrates the traces of vertical wrist position, vertical wrist velocity and grasp aperture over time for 8 consecutive reach-to-grasp movements with the replanted and healthy hand. Both patients showed marked differences between the healthy and replanted hand with smoother and more regular movement traces accompanying the unaffected compared to the replanted hands. In terms of the individual movement components of the reach-to-grasp task, the hand transport (represented by the vertical wrist position and wrist velocity) was less impaired than the distal component (represented by the grasp aperture formation), which was more variable in both spatial and temporal movement characteristics (cf. Fig. 3). Furthermore, the movement parameters for the replanted hand of patient JH were more similar to his healthy one as compared to patient GM.

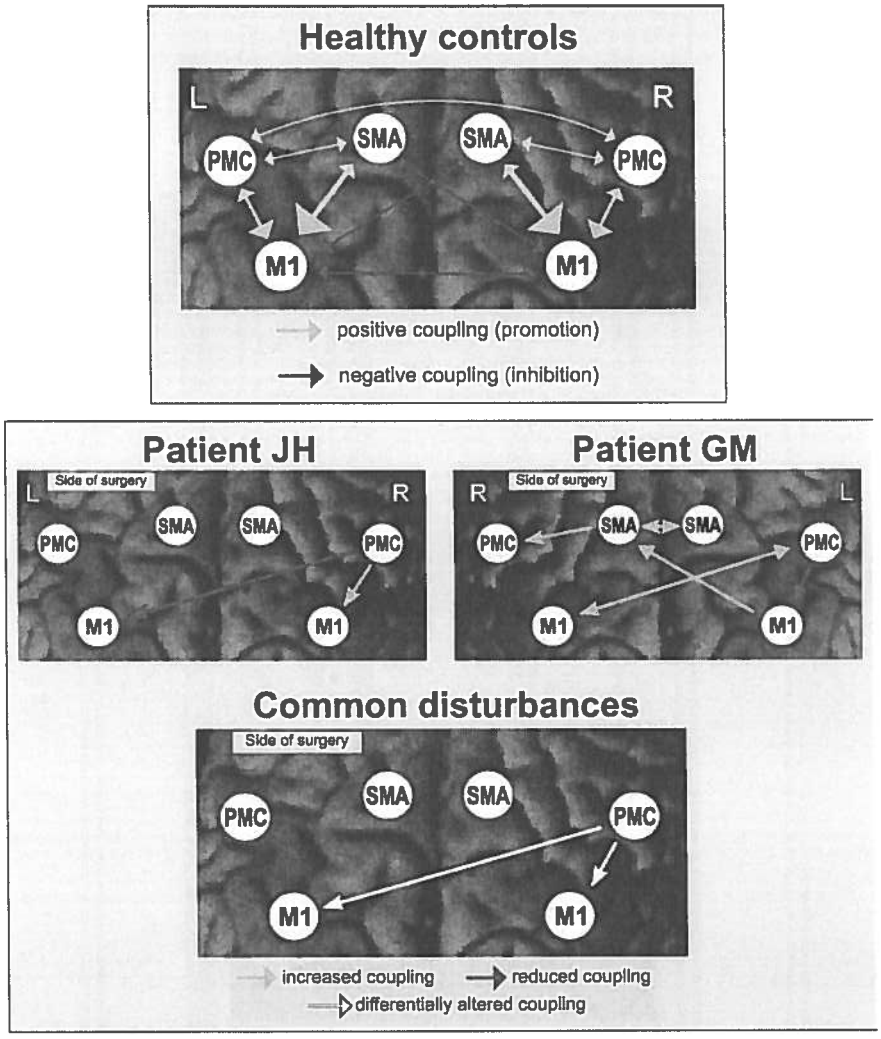

Fig. 4. Top panel: Regions of interest selected for estimating cortical connectivity shown on a surface rendering of the MNI single subject template. Displayed regions were significant at $p<0.05$ (corrected) in an *F*-contrast testing for the effects of interest, that is, regions where hand task-related variance was significantly greater than noise. To the right the intrinsic connectivity in healthy controls ($N=14$) as estimated by means of dynamic causal modelling is displayed. Reciprocal connectivity is assumed for the 6 motor regions, while visual input is provided via left and right V5 into all 4 premotor regions. Coupling parameters indicate connection strength, which are coded for size and colour. Positive coupling (green arrows) suggest a facilitation, whereas negative coupling (red arrows) can be interpreted as neural inhibition. Bottom panel: Differences in intrinsic connectivity between the two patients and the control group. Only those connections whose strength was significantly different ($p<0.05$ corrected) from those of the controls in a two-sample *T*-test are displayed. Green arrows denote coupling parameters which were significantly higher (more positive) as compared to normal subjects, red arrows those significantly lower, i.e., more negative. In the synoptical panel in the bottom row, white arrows indicate those connections which were significantly altered in both patients but effect changes in opposite directions. (For interpretation of the references to colour in this figure legend, the reader is referred to the web version of this article.)

Please cite this article as: Eickhoff, S.B., et al., Central adaptation following heterotopic hand replantation probed by fMRI and effective connectivity analysis, Exp. Neurol. (2008), doi:10.1016/j.expneurol.2008.03.025

Table 1 summarises the average values (+standard deviation) of peak lift position, movement time, peak wrist velocity, peak grasp aperture, peak velocity of grasp aperture and time of peak grasp aperture in percentage of movement time for reach-to-grasp movements with both hands in both hand replantation patients (Table 1). As mentioned above, peak wrist velocity and movement time of the wrist in the Z-axis is used to describe the transport component of the task. Movement time was shortest with healthy hands in both patients. However, peak wrist velocity was higher in the replanted hand of JH. For the distal component, peak grasp aperture and peak velocity of grasp aperture were lower/slower in the replanted hand. The time of peak grasp aperture expressed as a percentage of movement time (indicator of intact temporo-spatial coupling) deviated from the expected mean value of 50–70% as reported in healthy controls (Nowak et al., 2007) and also had a high standard deviation in patient GM. In summary, the kinematic motion analysis revealed general slowing of all movement components of the reach-to-grasp task at the replanted hand and a generally weaker performance of patient GM as compared to JH.

Intrinsic connectivity within the cortical motor network

The location of the analysed motor areas and their significant ($p<0.05$ corrected) intrinsic connections are summarised in the top panel of Fig. 4. In this context, "intrinsic" refers to interactions among brain regions which are not task-dependent and hence represent the constant part of the inter-regional connectivity. In healthy controls, intrinsic coupling was symmetrically organised across hemispheres with prominent positive influence of ipsilateral SMA and PMC on M1 activity. In contrast, all *transcallosal* pathways (except the PMC–PMC coupling) exerted a significant negative influence on their target area (Fig. 4, top).

In comparison, both patients showed a significantly ($p<0.05$ corrected) altered coupling between the PMC contralateral to the operated hand and both M1 cortices (bottom panel of Fig. 4). The nature of these changes, however, differed between them, as JH showed a significantly increased (positive) coupling between PMC contralateral to the operated hand and the M1 on the same hemisphere. In contrast, the transcallosal coupling to contralateral M1, which was (insignificantly) negative in controls, indicated a much more negative effect (stronger inhibition) in patient JH. In the second patient (GM), the opposite pattern was observed (Fig. 4): GM showed a significantly decreased input from PMC to the M1 cortex of the same side, while the coupling to M1 on the side of surgery was significantly enhanced, i.e., more positive. In contrast to the negative coupling between both SMA regions in the control group, patient GM experienced a significantly increased coupling between the supplementary motor areas in both hemispheres. Furthermore, increased input from the SMA ipsilateral to the operated hand to the PMC on the same hemisphere and from M1 contralateral to the operated hand to the SMA of the opposite hemisphere were found (Fig. 4).

The motor network during voluntary hand movements — controls

Compared to rest (i.e., no movement), visually paced right or left hand movements activated a primarily contralateral network including M1, SMA, PMC, the secondary somatosensory (Eickhoff et al., 2006, 2007a) and extrastriate visual cortices, while bilateral hand movements resulted in a symmetric activation of the aforementioned areas (Fig. 5). Modelling the effective connectivity underlying unilateral

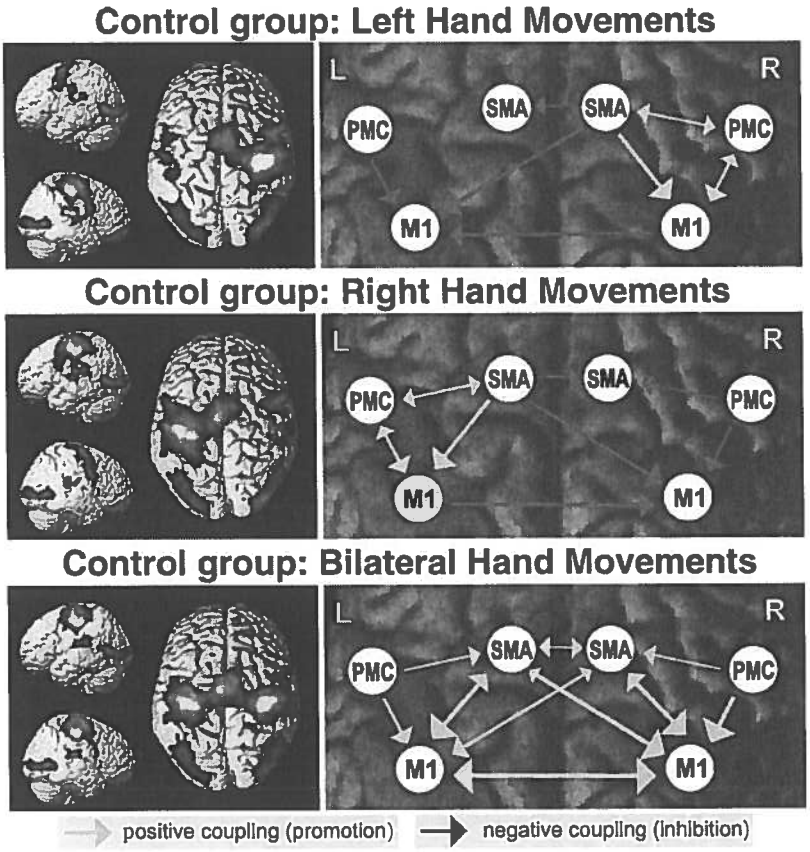

Fig. 5. Cortical activation (increases relative to resting state baseline) and significant ($p<0.05$ corrected) and modulatory effects on effective connectivity between cortical motor areas sustaining visually paced hand movements in healthy control subjects ($N=14$). Arrows indicate significantly modulated pathways ($p<0.05$, corrected) for right, left and bilateral hand movements (green: facilitation, red: inhibition). (For interpretation of the references to colour in this figure legend, the reader is referred to the web version of this article.)

Please cite this article as: Eickhoff, S.B., et al., Central adaptation following heterotopic hand replantation probed by fMRI and effective connectivity analysis, Exp. Neurol. (2008), doi:10.1016/j.expneurol.2008.03.025

hand movements revealed a significantly increased (positive) coupling between M1, PMC and SMA contralateral to the movement. In contrast, all connections towards and within the opposite (ipsilateral) hemisphere were significantly inhibited (Fig. 5). This was most noticeable in the ipsilateral M1 which received inhibitory input from contralateral M1, SMA and ipsilateral PMC. Finally, bilateral in-phase hand movements resulted in a symmetric significant increase in the connectivity both within and across hemispheres (Fig. 5).

The motor network during voluntary hand movements — patient JH

Movement of the operated left hand resulted in significantly increased activity in the right (contralateral) M1 cortex of JH as compared to controls. Regions where neural activity was significantly lowered were not observed. DCM analysis revealed that the contralateral (right) M1 cortex was subjected to both positively and negatively altered connectivity. The PMC contralateral to the operated hand, which was more strongly driven by the visual pacing cue most likely via a subcortical loop involving the basal ganglia or cerebellum, exerted a significantly increased input in this area (M1) on top of the already amplified intrinsic positive coupling (Fig. 6). On the other hand, M1 contralateral to the operated hand also received stronger transcallosal inhibitory input from PMC and M1. In summary, the net effects of these altered coupling parameters resulted in an increased M1 activity as evident from the comparison with the control population. When JH moved the right (non-operated) hand, no increased activity relative to controls was observed. There were, however, significantly more negative (inhibitory) influences from PMC and M1 of the left hemisphere to the right PMC, which resulted in significantly reduced activity in this region as compared to controls. In-phase movements of both hands resulted in a significantly more negative coupling from left M1 to right (contralateral to the operated hand) SMA as compared to controls. Consequently, the activity of the SMA contralateral to the operated hand was significantly reduced (Fig. 6).

The motor network during voluntary hand movements — patient GM

When GM moved his healthy left hand, disturbances in the cortical motor network were very similar to those observed when JH moved his healthy hand. In particular, in this patient there were significantly more inhibitory influences from PMC and M1 on the right (contralateral) hemisphere to left PMC (Fig. 7). However, as the latter area was at the same time more strongly driven by the visual cueing (which was not the case in JH), there was no significant net increase or decrease in

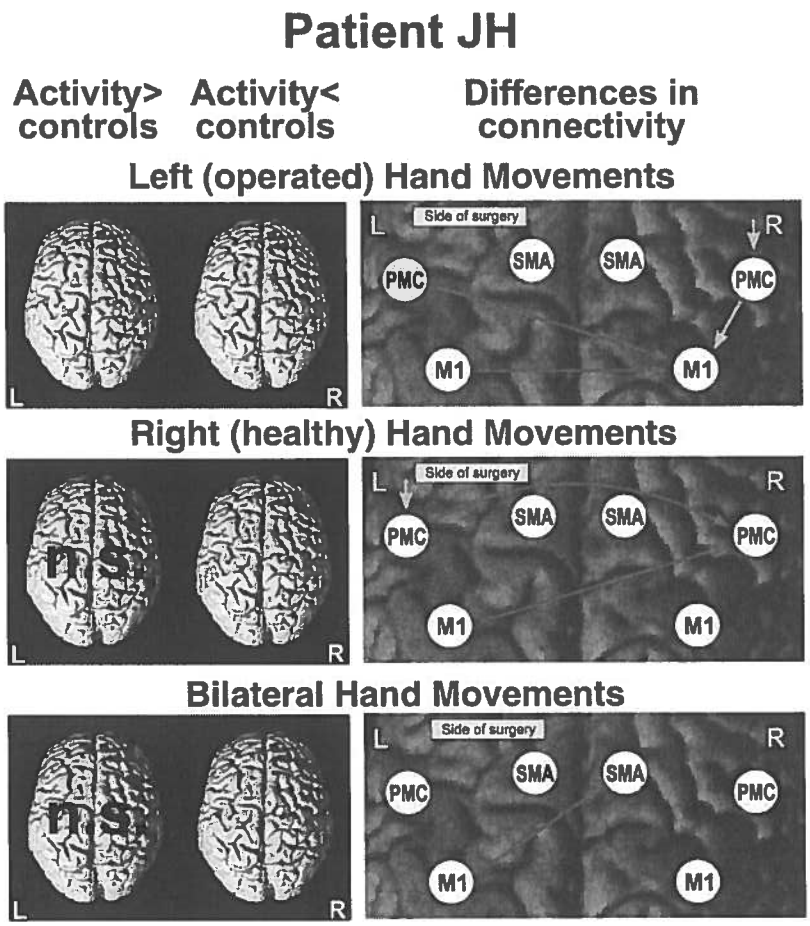

Fig. 6. Differences in activation (as assessed by an ANOVA on the parameter estimates from the first level analysis) and modulatory effects (as assessed by inference on the coupling parameters derived from the dynamic causal modelling) between patient JH and the control group. Differences in activation were tested separately in both directions (activity of JH > activity in controls and vice versa) and are displayed on the left [$p<p<0.001$ (unc.) with an extended threshold of $k=20$ voxels]. In the connectivity panels to the right, green arrows denote coupling parameters which were significantly higher (more positive) compared to normal subjects, red arrows those significantly lower, i.e., more negative (tests on parameters reported at $p<0.05$, corrected for multiple comparisons). The single arrows associated with PMC reflect significant differences in the context-dependent modulation of effective connectivity from V5 to the PMC between the respective patient and the controls (cf. Fig. 2, Table 2). These context-dependent modulations, which implicitly also capture the influence of putative subcortical relay structures, such as the basal ganglia or the cerebellum represent the increase in driving input into the premotor cortex in the presence of the respective task condition as opposed to resting baseline. (For interpretation of the references to colour in this figure legend, the reader is referred to the web version of this article.)

Please cite this article as: Eickhoff, S.B., et al., Central adaptation following heterotopic hand replantation probed by fMRI and effective connectivity analysis, Exp. Neurol. (2008), doi:10.1016/j.expneurol.2008.03.025

Table 2

Connection	Intrinsic connectivity			Modulation by left hand movement		
	Controls	JH	GM	Controls	JH	GM
$V5_L \rightarrow PMC_L$	0.09±0.08	0.17	0.21	0.00±0.03	−0.09	**0.10**
$V5_L \rightarrow PMC_R$	0.11±0.06	0.06	0.03	0.01±0.03	**0.14**	0.00
$V5_L \rightarrow SMA_L$	0.03±0.11	0.11	0.01	−0.14±0.06	−0.06	−0.01
$V5_L \rightarrow SMA_R$	0.08±0.11	0.07	0.05	0.09±0.06	−0.00	−0.00
$V5_R \rightarrow PMC_L$	0.12±0.06	0.19	0.06	0.00±0.05	−0.16	−0.01
$V5_R \rightarrow PMC_R$	0.16±0.10	0.18	0.05	0.02±0.04	**0.25**	−0.00
$V5_R \rightarrow SMA_L$	0.10±0.09	0.11	0.05	−0.18±0.09	−0.10	0.00
$V5_R \rightarrow$ SMA R	0.07±0.10	0.10	0.08	0.10±0.05	−0.00	0.00
$PMC_L \rightarrow PMC_R$	0.13±0.07	−0.01	0.11	0.03±0.03	−0.04	−0.02
$PMC_L \rightarrow SMA_L$	0.13±0.08	0.23	0.00	−0.02±0.04	−0.02	−0.03
$PMC_L \rightarrow SMA_R$	0.07±0.06	0.09	0.01	0.03±0.03	0.00	−0.03
$PMC_L \rightarrow M1_L$	0.20±0.10	0.31	**−0.36**	−0.06±0.05	−0.02	−0.06
$PMC_L \rightarrow M1_R$	0.12±0.10	0.08	**0.56**	0.07±0.03	**−0.07**	0.01
$PMC_R \rightarrow PMC_L$	0.12±0.07	−0.07	0.28	0.03±0.04	−0.06	**−0.08**
$PMC_R \rightarrow SMA_L$	0.15±0.11	−0.06	0.40	−0.03±0.05	−0.02	0.06
$PMC_R \rightarrow SMA_R$	0.11±0.08	0.07	0.36	0.05±0.04	−0.01	0.06
$PMC_R \rightarrow M1_L$	0.21±0.12	**−0.15**	0.38	−0.09±0.06	−0.11	−0.05
$PMC_R \rightarrow M1_R$	0.18±0.12	**0.47**	0.20	0.09±0.06	**0.30**	0.01
$SMA_L \rightarrow PMC_L$	0.11±0.08	0.29	0.19	0.01±0.02	−0.00	−0.06
$SMA_L \rightarrow PMC_R$	0.13±0.10	−0.02	0.45	0.01±0.03	−0.03	0.06
$SMA_L \rightarrow SMA_R$	−0.03±0.06	0.06	**0.35**	0.01±0.04	0.00	0.06
$SMA_L \rightarrow M1_L$	0.55±0.16	0.34	0.40	0.01±0.05	−0.00	−0.04
$SMA_L \rightarrow M1_R$	−0.08±0.08	0.04	0.11	0.01±0.06	−0.05	0.01
$SMA_R \rightarrow PMC_L$	0.07±0.04	0.07	0.19	0.04±0.04	−0.02	−0.06
$SMA_R \rightarrow PMC_R$	0.10±0.07	0.06	**0.42**	0.05±0.04	0.03	0.06
$SMA_R \rightarrow SMA_L$	−0.03±0.07	0.04	**0.37**	−0.03±0.06	−0.01	0.06
$SMA_R \rightarrow M1_L$	−0.10±0.13	0.07	0.34	−0.09±0.05	−0.03	−0.04
$SMA_R \rightarrow M1_R$	0.54±0.19	0.11	0.13	0.10±0.04	0.05	0.01
$M1_L \rightarrow PMC_L$	0.10±0.07	0.37	−0.04	0.00±0.02	0.01	−0.01
$M1_L \rightarrow PMC_R$	0.13±0.09	−0.05	0.42	0.00±0.03	−0.10	0.07
$M1_L \rightarrow SMA_L$	0.35±0.14	0.19	0.40	0.00±0.02	−0.02	0.07
$M1_L \rightarrow SMA_R$	−0.04±0.07	0.05	**0.36**	0.01±0.04	0.01	0.07
$M1_L \rightarrow M1_R$	−0.12±0.08	−0.03	−0.19	0.00±0.05	**−0.16**	0.01
M1 R → PMC_L	0.07±0.06	−0.00	**0.47**	0.04±0.05	−0.04	**−0.07**
M1 R → PMC_R	0.11±0.09	0.32	0.05	0.06±0.05	0.15	−0.02
M1 R → SMA_L	−0.02±0.06	−0.01	−0.04	−0.01±0.06	0.01	−0.03
M1 R → SMA_R	0.34±0.17	0.07	−0.03	0.05±0.04	−0.01	−0.03
M1 R → $M1_L$	−0.10±0.09	−0.05	−0.37	−0.07±0.05	−0.06	−0.07

Connection	Modulation by right hand movement			Modulation by bilateral hand movement		
	Controls	JH	GM	Controls	JH	GM
$V5_L \rightarrow PMC_L$	0.02±0.02	**0.14**	**0.08**	−0.00±0.02	0.09	−0.04
$V5_L \rightarrow PMC_R$	0.02±0.03	−0.14	0.04	0.01±0.02	0.01	−0.02
$V5_L \rightarrow SMA_L$	0.07±0.03	0.10	0.04	0.06±0.05	0.04	−0.02
$V5_L \rightarrow SMA_R$	−0.13±0.07	0.02	0.07	0.06±0.04	0.01	−0.01
$V5_R \rightarrow PMC_L$	0.02±0.03	**0.16**	**0.07**	0.00±0.06	0.14	−0.04
$V5_R \rightarrow PMC_R$	0.03±0.04	−0.16	0.04	0.01±0.03	0.01	−0.02
$V5_R \rightarrow SMA_L$	0.11±0.03	0.12	0.04	0.09±0.07	0.07	−0.01
$V5_R \rightarrow$ SMA R	−0.18±0.09	0.02	0.06	0.10±0.09	0.01	−0.01
$PMC_L \rightarrow PMC_R$	0.03±0.03	**−0.14**	−0.01	0.02±0.03	0.05	−0.00
$PMC_L \rightarrow SMA_L$	0.04±0.03	0.03	−0.02	0.06±0.03	0.08	−0.00
$PMC_L \rightarrow SMA_R$	−0.04±0.03	−0.05	0.01	0.05±0.03	−0.03	−0.03
$PMC_L \rightarrow M1_L$	0.06±0.03	0.10	**−0.13**	0.08±0.04	0.18	−0.05
$PMC_L \rightarrow M1_R$	−0.07±0.04	−0.10	0.09	0.09±0.04	0.10	−0.02
$PMC_R \rightarrow PMC_L$	0.02±0.02	−0.01	−0.03	0.01±0.05	0.06	−0.00
$PMC_R \rightarrow SMA_L$	0.05±0.04	0.01	−0.04	0.07±0.04	0.02	0.06
$PMC_R \rightarrow SMA_R$	−0.05±0.04	0.04	−0.03	0.06±0.04	−0.01	0.04
$PMC_R \rightarrow M1_L$	0.08±0.05	−0.02	0.06	0.11±0.05	0.06	0.02
$PMC_R \rightarrow M1_R$	−0.08±0.05	0.02	−0.06	0.12±0.05	0.03	0.00
$SMA_L \rightarrow PMC_L$	0.04±0.03	0.05	−0.02	0.01±0.06	0.12	−0.00
$SMA_L \rightarrow PMC_R$	0.06±0.05	−0.10	−0.02	0.03±0.05	0.03	0.05
$SMA_L \rightarrow SMA_R$	−0.05±0.04	−0.03	−0.02	0.07±0.04	−0.02	0.05
$SMA_L \rightarrow M1_L$	0.10±0.05	0.07	0.06	0.12±0.04	0.11	0.03
$SMA_L \rightarrow M1_R$	−0.09±0.04	−0.07	−0.06	0.13±0.05	0.06	0.01
$SMA_R \rightarrow PMC_L$	−0.01±0.02	0.03	−0.01	0.01±0.03	0.04	−0.00
$SMA_R \rightarrow PMC_R$	−0.02±0.03	−0.03	−0.02	0.02±0.03	0.01	0.04
$SMA_R \rightarrow SMA_L$	−0.01±0.03	0.02	−0.03	0.06±0.03	0.02	0.05
$SMA_R \rightarrow M1_L$	−0.02±0.04	0.03	0.04	0.11±0.05	0.04	0.02
$SMA_R \rightarrow M1_R$	0.01±0.04	−0.03	−0.03	0.12±0.05	0.02	0.00
$M1_L \rightarrow PMC_L$	0.04±0.03	0.03	0.00	0.01±0.06	0.16	−0.00
$M1_L \rightarrow PMC_R$	0.07±0.05	**−0.09**	−0.01	0.03±0.05	0.05	0.05
$M1_L \rightarrow SMA_L$	0.06±0.07	−0.01	−0.03	0.08±0.05	0.06	0.06

Table 2 (*continued*)

Connection	Modulation by right hand movement			Modulation by bilateral hand movement		
	Controls	JH	GM	Controls	JH	GM
$M1_L \rightarrow SMA_R$	−0.04±0.05	−0.07	−0.03	0.07±0.04	**−0.03**	0.07
$M1_L \rightarrow M1_R$	−0.07±0.05	−0.06	−0.14	0.13±0.05	0.08	0.02
M1 R → PMC_L	−0.01±0.02	0.00	−0.05	0.02±0.03	0.08	−0.00
M1 R → PMC_R	−0.02±0.03	0.02	−0.02	0.04±0.04	0.02	−0.00
M1 R → SMA_L	−0.02±0.04	0.01	−0.02	0.07±0.03	0.03	**−0.01**
M1 R → SMA_R	0.00±0.02	0.03	0.00	0.08±0.06	−0.02	−0.03
M1 R → $M1_L$	−0.03±0.04	−0.00	**−0.13**	0.11±0.05	0.07	−0.03

Coupling parameters for the connections summarised in Fig. 2 as estimated by DCM in the 14 control subjects (mean±standard deviation) and the two investigated patients. Bold numbers indicate significant differences between patients and control subjects ($p<0.05$, Bonferroni-corrected for multiple comparisons, cf. Figs. 4–8).

brain activity as compared to the control group. When GM moved the right, replanted hand, both similarities and differences in the connectivity disturbances of JH were evident. Similarly, GM showed a significantly stronger negative influence from M1 ipsilateral to the replantation in the contralateral M1 and an increased driving influence of the visual pacing of the PMC on the same side (Fig. 7). The connectivity from the PMC contralateral to the operated hand and M1 on the same hemisphere was also significantly altered, but in contrast to the increased connectivity observed in JH, coupling was reduced in GM. As a result of these inhibitory influences, the activity in the M1 contralateral to the operated hand was significantly reduced relative to the controls. Relative to healthy subjects, in-phase movements of both hands resulted in a significantly stronger inhibition of right M1 on left (=contralateral to the operated hand) SMA, and hence a significantly reduced activity of the latter area (Fig. 7).

The motor network during voluntary hand movements — synopsis

Healthy hand movements

Compared to healthy controls, there was a significantly greater negative influence onto the PMC contralateral to the operated hand being exerted from the PMC and the M1 of the opposite hemisphere in both patients. Differences between the patients were observed with respect to the driving input, which was increased on the PMC ipsilateral to the operated hand in JH and on the opposite side in GM (Fig. 8, top).

Operated hand movements

In both patients the motor cortex contralateral to the replanted (active) hand was pathologically inhibited by the M1 cortex of the opposite hemisphere. Additionally, there was a significantly increased driving input into the PMC contralateral to the replanted hand. The coupling between PMC contralateral to the replanted hand and M1 on the same hemisphere, however, was significantly increased in JH but decreased in GM (Fig. 8, middle).

Bilateral hand movements

Moving both hands in-phase both JH and GM showed a significantly enhanced negative influence of M1 ipsilateral to the operated hand onto the SMA contralateral to surgery (Fig. 8, bottom).

Discussion

In this study we used fMRI and dynamic causal modelling to examine the adaptation of the cortical motor network formed by areas M1 (primary motor cortex), PMC (ventral premotor cortex) and SMA (supplementary motor area) in two patients following heterotopic hand replantation. Additional kinematic analysis indicated a general slowing of the various movement components of reach-to grasp movements for the replanted hand, especially for patient GM. In comparison with healthy controls the imaging data demonstrated that both patients

Please cite this article as: Eickhoff, S.B., et al., Central adaptation following heterotopic hand replantation probed by fMRI and effective connectivity analysis, Exp. Neurol. (2008), doi:10.1016/j.expneurol.2008.03.025

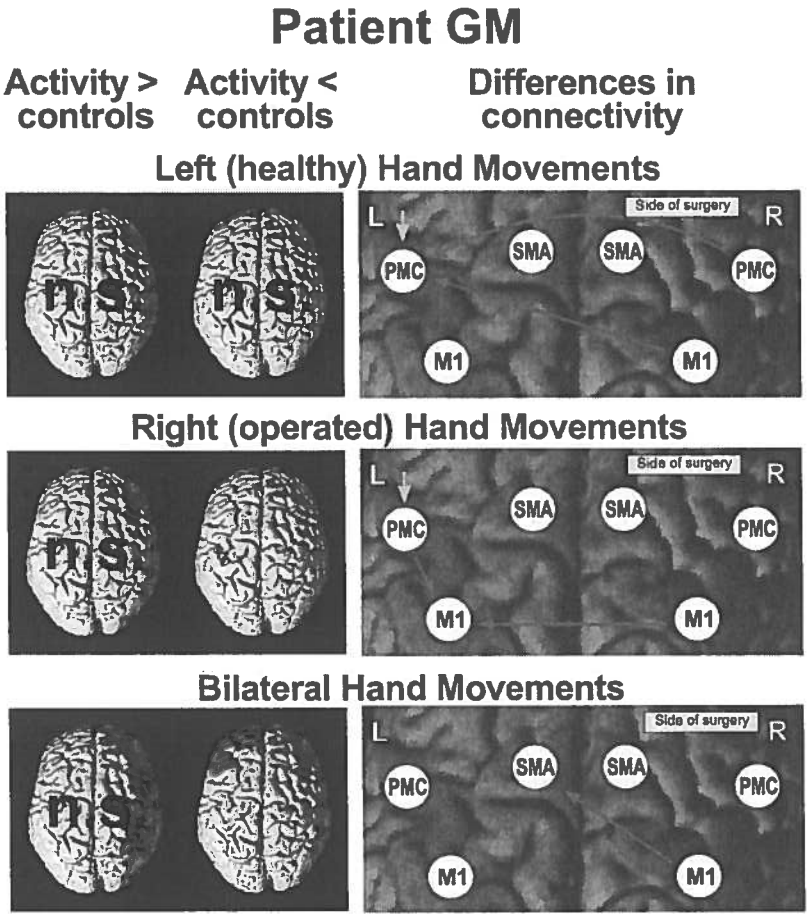

Fig. 7. Differences in activation (as assessed by an ANOVA on the parameter estimates from the first level analysis) and modulatory effects (as assessed by inference on the coupling parameters derived from the dynamic causal modelling) between patient GM and the control group. Differences in activation were tested separately in both directions (activity of JH > activity in controls and vice versa) and are displayed on the left [$p<p<0.001$ (unc.) with an extend threshold of $k=20$ voxels]. In the connectivity panels to the right, green arrows denote coupling parameters which were significantly higher (more positive) compared to normal subjects, red arrows those significantly lower, i.e., more negative (tests on parameters reported at $p<0.05$, corrected for multiple comparisons). The single arrows associated with PMC reflect significant differences in the context-dependent modulation of effective connectivity from V5 to the PMC between the respective patient and the controls (cf. Fig. 2, Table 2). These context-dependent modulations, which implicitly also capture the influence of putative subcortical relay structures, such as the basal ganglia or the cerebellum represent the increase in driving input into the premotor cortex in the presence of the respective task condition as opposed to resting baseline. (For interpretation of the references to colour in this figure legend, the reader is referred to the web version of this article.)

showed significant changes in cortical activation during movements of the replanted hand, which was accompanied by changes in inter-regional coupling.

Technical aspects

The idea behind DCM is to consider the brain as a deterministic nonlinear system that is subject to known inputs (either provided by direct sensory stimulation or by contextual influences such as task settings) which produces externally assessable outputs such as the BOLD signal measured in the present study. The effective connectivity within this dynamic system is expressed in terms of coupling between unobservable brain states (e.g., the modelled neuronal activity in the different regions comprised in the model). These neuronal state models are then linked to the measured functional response (i.e., a change in the BOLD response) via a biophysically validated hemodynamic response model (Friston et al., 2003). The objective of DCM analyses is to estimate these neuronal coupling parameters based on perturbing the system trough experimental manipulation, i.e., by presenting the subjects with different tasks, while measuring the evoked effects on the BOLD time-series of the respective regions included in the model. This approach has several advantages over other methods for estimating effective connectivity such as structural equation modelling (SEM) and multivariate autoregressive processes (MAR). In these analyses, there is no designed perturbation and the inputs are treated as unknown and stochastic; consequently the information about the experimental setup and timing is ignored. Moreover, MAR and related approaches such as coherence analysis do not only assume that the system is driven by stochastic effects, but are restricted to linear interactions and, in the case of correlation or coherence analyses, suffer from insensitivity to directional and timing information of neural connectivity. SEM furthermore assumes further instantaneous realisation of all interactions, rendering this approach to a variant of correlation analysis as opposed to a dynamic time-series model.

In summary, DCM thus differs from alternative approaches for testing effective connectivity by explicitly modelling the nonlinear dynamic aspects of neuronal interactions which are driven through known, experimentally designed perturbations and then related to the measured BOLD signal via a biophysically validated forward hemodynamic model (Friston et al., 2003).

Analysis of activation vs. connectivity

We assessed differences between patients and controls both in terms of fMRI contrasts (activation) and inter-regional coupling (connectivity). A comparison of the obtained results indicated a good congruency between these two complementary analyses. For example, in both patients the increased inhibition exerted by M1 ipsilateral to the replanted

Please cite this article as: Eickhoff, S.B., et al., Central adaptation following heterotopic hand replantation probed by fMRI and effective connectivity analysis, Exp. Neurol. (2008), doi:10.1016/j.expneurol.2008.03.025

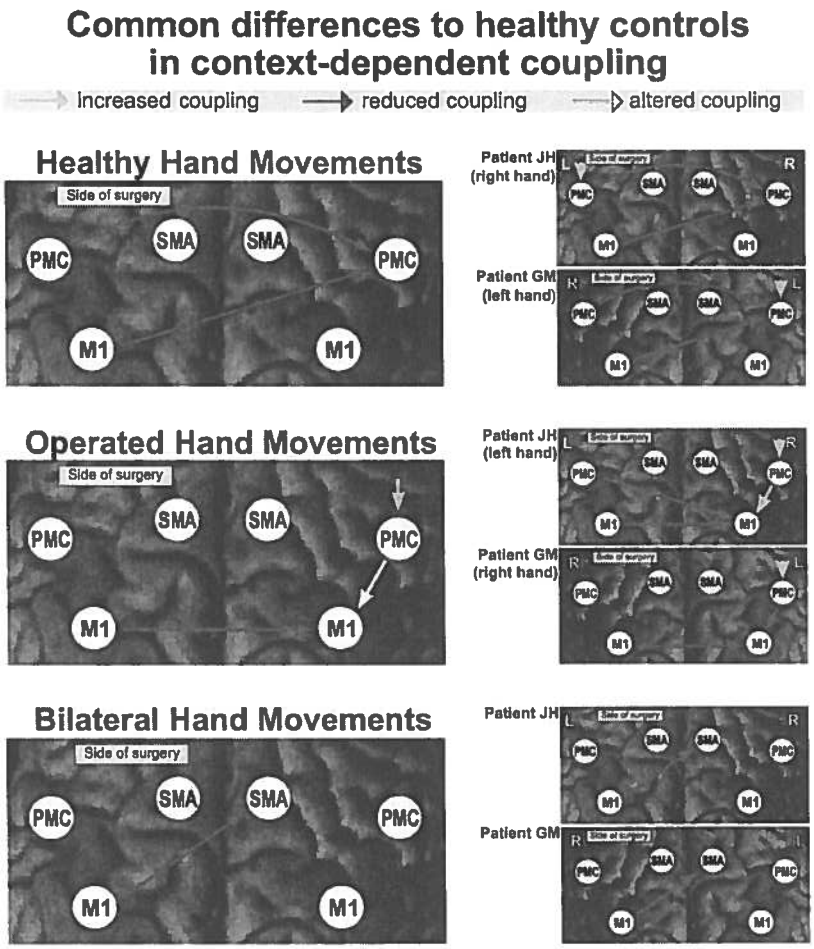

Fig. 8. Synopsis of changes in the cortical (i.e., central) motor network following heterotopic hand replantation (i.e, peripheral manipulation) in the two patients. Only connections whose strength was significantly different ($p<0.05$ corrected) from those of the controls are displayed. Green arrows denote coupling parameters which were significantly higher (more positive) compared to normal subjects, red arrows those significantly lower, i.e., more negative. White arrows indicate those connections which were significantly altered in both patients but effect changes in opposite directions. (For interpretation of the references to colour in this figure legend, the reader is referred to the web version of this article.)

hand on contralateral SMA estimated in the DCM analysis was reflected by decreased fMRI activation. However, not all significant changes in inter-regional coupling were found to correlate with significantly altered estimates of fMRI activation. A likely reason for the increased sensitivity of DCM to pathological changes is its explicit estimation of neuro-vascular parameters (Friston et al., 2003) accommodating differences in the hemodynamic response function between areas and subjects (Gitelman et al., 2003). The resulting connectivity estimates are thus (in contrast to the estimates of activation strengths in conventional fMRI analysis) independent of the accuracy-of-fit between the individual hemodynamic response and its canonical form. Moreover, analysing effective connectivity between cortical areas also permits the intrusion of characterising disturbances which may not result in net changes of activation strength, e.g., in the case of an area receiving increased promoting input from one region and increased inhibition from another.

Effective connectivity analyses may in fact provide an important and highly sensitive tool for the assessment of pathologically disturbed brain networks not only in group studies (Grefkes et al., 2007; Heim et al., in press) but also at the level of individual patients.

Effects of heterotopic hand replantation on cortical motor networks

Unfortunately, the number of patients recruited was limited even though our sample comprised of all patients who recovered hand function after heterotopic replantation as defined by the Biemer-criteria [replantation following complete disconnection of the distal limb (Biemer, 1977)]. The radical modifications of the musculoskeletal system sustaining the operated hand function in combination with the clinical outcome of regained behavioural capabilities nevertheless provide a unique insight in the adaptation of central motor control following peripheral changes. As summarised in Figs. 4 and 8, multiple connections showed pathologic intrinsic or task-dependent coupling in both patients representing cortical re-organisation following hand replantation. Some of these changes were congruent between patients, other connections, however, were disturbed in opposite directions.

Congruent alternations in motor connectivity

Both patients showed inhibition of PMC contralateral to the operated hand by both the PMC and M1 of the opposite hemisphere when the healthy hand was moved. This change can be interpreted as an enhanced suppression of influence from the "affected" hemisphere (i.e., that controlling the replanted hand) on the control of the healthy hand (Friston et al., 2003; Grefkes et al., 2007; Stephan et al., 2004). Most likely this mechanism serves to prevent the disturbance of physiological motor execution (Chouinard and Paus, 2006; Rizzolatti et al., 2002) by the PMC which has undergone adaptive changes to cope with the effects of surgical changes of the peripheral motor effectors. A similar pathophysiology may underlie the inhibition of SMA contralateral to the operated hand by the opposite M1 when both hands had to be moved in-phase. As the role of the SMA regions and their interaction in the coordination of bilateral hand movements is

Please cite this article as: Eickhoff, S.B., et al., Central adaptation following heterotopic hand replantation probed by fMRI and effective connectivity analysis, Exp. Neurol. (2008), doi:10.1016/j.expneurol.2008.03.025

well established (Chouinard and Paus, 2006; Halsband and Lange, 2006; Rizzolatti and Luppino, 2001), the observed negative feedback on the SMA contralateral to the replanted hand may again be regarded as a suppression of influence exerted by the adapted hemisphere. This process, in turn, enables the hemisphere controlling the healthy hand to take the lead in the initiation and control of the bilateral movement. To summarise, we may conclude that tasks involving movement of the healthy hand, either in isolation or in a bimanual task, lead to an increased (relative to controls) suppression of activity in the hemisphere contralateral to the replant, limiting its influence in the cortical motor network (Chouinard and Paus, 2006; Gerloff and Andres, 2002; Rizzolatti et al., 2002).

When the patients moved their operated hand, both of them showed an increased driving influence of the visual pacing on the PMC contralateral to the operated side. As already noted, the estimated coupling parameters represent the effective net influence of cue-evoked activity on the PMC (Friston et al., 2003) implicitly including influences of presumed subcortical relay structures, such as the basal ganglia or cerebellum (Halsband and Lange, 2006; Taniwaki et al., 2006). Most likely this increased driving input into the PMC reflects the additional effort needed by the patients to move their replanted hand in comparison to the (low) demands imposed by stereotypic hand movements in healthy subjects. Increased recruitment of the contralateral PMC, a key structure for preparing and updating motor programs which are to be executed by M1 (Rizzolatti et al., 2002; Vogt et al., 2007), may hence represent a direct correlate of the adaptation required to effectively control the operated hand in spite of its unphysiological anatomy. In further agreement with this view, therapy-induced improvements in upper limb function in chronic stroke patients are associated with increased activation dorsal premotor cortex contralateral to the impaired hand (Johansen-Berg et al., 2002).

However, in the same task (operated hand movement) we also observed a pathological negative influence of the ipsilateral M1 on its active contralateral counterpart in both patients. That is, in contrast to healthy subjects, JH and GM failed to modulate the intrinsic balance of reciprocal inhibition between the primary motor cortices in favour of the one contralateral to the movement. Interestingly, identical pathological alternation has been described in patients following subcortical stroke which were asked to perform the same paradigm as employed in this study with their paretic hand (Grefkes et al., 2007). Transcranial stimulation (TMS) data obtained in healthy subjects showed that under physiological conditions, both M1 exhibit a mutual inhibitory influence on each other (Ferbert et al., 1992; Wassermann et al., 1991), which is reflected in the present fMRI-DCM data by showing a strong negative coupling between both M1. Anatomical tracing studies in monkeys imply that such transcallosal M1–M1 interactions are only present in those primate species exhibiting manual skills with relatively independent finger movements (Gould et al., 1986; Rouiller et al., 1994). Likewise, transcallosal inhibition is thought to prevent interference from M1 of the opposite hemisphere, for example mirror movements of the hands (Mayston et al., 1999). In human stroke patients, movements of the paretic hand were shown to be associated with increased inhibitory influences from the unaffected motor cortex (Duque et al., 2005; Murase et al., 2004), and reducing these influences by means of inhibitory TMS over contralesional M1 may indeed ameliorate the motor skills of the stroke affected hand (Nowak et al., in press; Takeuchi et al., 2005). The findings of the present study suggest, that also following heterotopic hand replantation similar (unphysiological) inhibitory influences may be present and contribute to the behavioural impairment of the patients. Suppressing these inhibitory influences, e.g., by means of low-frequency repetitive TMS as employed in stroke patients, might assist understanding of the nature of these interactions, and perhaps offer an additional therapy option to promote recovery of function.

Diverging alternations in motor connectivity

The most striking differences between the two patients were evident in the influences exerted by the PMC contralateral to the replanted hand onto the two primary motor cortices. In the case of JH, this area showed an increased (relative to controls) positive, i.e., promoting, intrinsic influence on M1 in the same hemisphere and an increased inhibitory intrinsic influence on M1 ipsilateral to surgery. In other words, in patient JH, the intrinsic balance of the motor network was shifted towards the hemisphere controlling the replanted hand. In the second patient, GM, the opposite was observed. Here the M1 contralateral to the operated hand was suppressed while M1 on the other hemisphere received enhanced input, resulting in an imbalance favouring the hemisphere controlling the healthy hand. Moreover, movement of the operated hand resulted in a significantly increased coupling between PMC contralateral to the operated, i.e., active hand onto M1 in the same hemisphere in the case of JH (relative to controls) and a decreased one in patient GM. Therefore, rather than counteracting the intrinsic imbalances, active movement of the operated hand caused them become even more pronounced. Importantly, these differences in effective connectivity also had a correlate in behavioural performance, as kinematic analysis revealed a more pronounced deficit in replanted hand motor skills in patient GM, whose motor cortex on the hemisphere contralateral to the replanted hand was experiencing increased tonic (intrinsic connectivity) and phasic (context-dependent modulation) inhibition.

These differences in cortical motor network adaptation and the ensuing proficiency in replanted hand use most likely reflect the diverging post-operative history of the two patients. Patient GM was operated on 18 years ago but subsequently developed an extended haematoma requiring broad surgical revision with split-thickness skin graft for defect coverage. These complications resulted in long-term immobilisation of the replanted hand and a conservative approach to rehabilitation. Although the result was later described as satisfactory (Windhager et al., 1995), manual abilities remained severely limited to basic grip and hold functions. Consequently GM almost exclusively used his healthy left hand for fine motor tasks before his hand was re-operated 17 years later. In contrast, the operation of patient JH, which was performed 2 years ago, yielded a very good initial result. Therefore intense rehabilitative exercise of the replanted hand could be commenced early and consistently following the surgery (Piza-Katzer et al., 2006). This meticulous training regimen resulted in a remarkable recovery of hand function, which now allows JH to fully use his replanted left hand in everyday life. We are now able to show that these differences in functional recovery, which were confirmed by kinematic analysis, apparently derived from diverging adaptive changes in cortical motor controls induced by post-operative rehabilitation (Lundborg, 2000); JH, who exercised and used his replanted hand early and frequently, shows an increased recruitment and enhanced coupling of the contralateral primary motor cortex both at rest and when moving the replanted hand and regained remarkable manual skills with his replant. In contrast, GM, who had to be immobilised after surgery and subsequently used his operated hand only occasionally as an auxiliary tool, shows mainly inhibitory couplings towards M1 contralateral to the operated side and a poorer proficiency in his replanted hand.

Conclusions and further research

The analysis of the two patients following heterotopic hand replantation allowed the assessment of adaptive changes in central motor control both at the level of cortical activation (using fMRI) and inter-regional coupling (using DCM). It could be shown that surgically manipulated peripheral anatomy and the subsequent recovery of function are reflected in a functional re-organisation of the cortical network architecture. Moreover, inter-individual differences in post-operative rehabilitation not only affected the level of regained motor

Please cite this article as: Eickhoff, S.B., et al., Central adaptation following heterotopic hand replantation probed by fMRI and effective connectivity analysis, Exp. Neurol. (2008), doi:10.1016/j.expneurol.2008.03.025

function but also resulted in distinct patterns of cortical network adaptation. The present study demonstrates that DCM is a promising tool to indicate pathological disturbances of effective connectivity at individual levels. Importantly, as discussed above, the differences noted between the two patients appear congruent to the rehabilitation outcome and hence should reflect a plastic adaptation to the different exercise regimen. Given the small sample of subjects available for analysis and the experimental constraints imposed by the fMRI setting, however, the correspondence between behavioural recovery (as measured by the kinematic analysis) could not be quantified in the present study. It should be noted, however, that such an analysis is generally feasible and was done for a group of subcortical stroke patients using the same paradigm and analysis methods. We were able to demonstrate that the strength of the negative coupling from ipsi- to contralateral M1 correlated with the maximum finger tapping frequency of the patients, indicating the potential of DCM for investigating pathophysiological mechanisms at a group level (Grefkes et al., 2007). In the present study the same approach extends the inference concerning pathological network interactions to the level of individual patients and showed that the observed changes in effective connectivity may be related to the individual outcome of each patient.

One of the great remaining challenges for the future, however, is the integration of complex behavioural tasks with imaging data, which should represent a much better parameterisation of impairment and recovery than simple tasks like finger tapping or fist closure. Likewise, longitudinal studies following the dynamics of network reorganisation or systematic investigation into the changes of effective connectivity following different treatment/rehabilitation regimes still have to be performed. Nevertheless, we believe that functional neuroimaging and effective connectivity analyses permit the monitoring of plastic changes due to central or peripheral pathology and the subsequent recovery thereof. Such an approach may provide a valuable tool to understand, evaluate and qualitatively enhance the rehabilitation of motor function following central or peripheral tissue damage.

Acknowledgments

This Human Brain Project/Neuroinformatics research is funded by the National Institute of Biomedical Imaging and Bioengineering, the National Institute of Neurological Disorders and Stroke, the National Institute of Mental Health and the Deutsche Forschungsgemeinschaft (KFO-112), and the Brain Imaging Center West (BMBF 01GO0204).

References

Amunts, K., Malikovic, A., Mohlberg, H., Schormann, T., Zilles, K., 2000. Brodmann's areas 17 and 18 brought into stereotaxic space–where and how variable? NeuroImage 11, 66–84.
Ashburner, J., Friston, K.J., 2003. Rigid body registration, In: Frackowiak, R.S., Friston, K.J., Frith, C.D., Dolan, R.J., Price, C.J., Ashburner, J., Penny, W.D., Zeki, S. (Eds.), Human Brain Function, 2 ed. Academic Press, pp. 635–655.
Ashburner, J., Friston, K.J., 2005. Unified segmentation. NeuroImage 26, 839–851.
Biemer, E., 1977. Classification of total and subtotal amputations. Handchirurgie 9, 21–23.
Burton, H., Snyder, A.Z., Conturo, T.E., Akbudak, E., Ollinger, J.M., Raichle, M.E., 2002. Adaptive changes in early and late blind: a fMRI study of Braille reading. J. Neurophysiol. 87, 589–607.
Burton, H., Sinclair, R.J., McLaren, D.G., 2004. Cortical activity to vibrotactile stimulation: an fMRI study in blind and sighted individuals. Hum. Brain Mapp. 23, 210–228.
Chollet, F., Weiller, C., 1994. Imaging recovery of function following brain injury. Curr. Opin. Neurobiol. 4, 226–230.
Chouinard, P.A., Paus, T., 2006. The primary motor and premotor areas of the human cerebral cortex. Neuroscientist 12, 143–152.
Ding, Y., Kastin, A.J., Pan, W., 2005. Neural plasticity after spinal cord injury. Curr. Pharm. Des. 11, 1441–1450.
Duque, J., Hummel, F., Celnik, P., Murase, N., Mazzocchio, R., Cohen, L.G., 2005. Transcallosal inhibition in chronic subcortical stroke. NeuroImage 28, 940–946.
Eickhoff, S.B., Stephan, K.E., Mohlberg, H., Grefkes, C., Fink, G.R., Amunts, K., Zilles, K., 2005. A new SPM toolbox for combining probabilistic cytoarchitectonic maps and functional imaging data. NeuroImage 25, 1325–1335.
Eickhoff, S.B., Amunts, K., Mohlberg, H., Zilles, K., 2006. The human parietal operculum. II. Stereotaxic maps and correlation with functional imaging results. Cereb. Cortex 16, 268–279.
Eickhoff, S.B., Grefkes, C., Zilles, K., Fink, G.R., 2007a. The somatotopic organization of cytoarchitectonic areas on the human parietal operculum. Cereb. Cortex 17, 1800–1811.
Eickhoff, S.B., Paus, T., Caspers, S., Grosbas, M.H., Evans, A.C., Zilles, K., Amunts, K., 2007b. Assignment of functional activations to probabilistic cytoarchitectonic areas revisited. NeuroImage 36, 511–521.
Ferbert, A., Priori, A., Rothwell, J.C., Day, B.L., Colebatch, J.G., Marsden, C.D., 1992. Interhemispheric inhibition of the human motor cortex. J. Physiol. 453, 525–546.
Friston, K.J., Holmes, A.P., Price, C.J., Buchel, C., Worsley, K.J., 1999a. Multisubject fMRI studies and conjunction analyses. NeuroImage 10, 385–396.
Friston, K.J., Holmes, A.P., Worsley, K.J., 1999b. How many subjects constitute a study? NeuroImage 10, 1–5.
Friston, K.J., Harrison, L., Penny, W., 2003. Dynamic causal modelling. NeuroImage 19, 1273–1302.
Gerloff, C., Andres, F.G., 2002. Bimanual coordination and interhemispheric interaction. Acta Psychol. (Amst.) 110, 161–186.
Geyer, S., 2003. The Microstructural Border Between the Motor and the Cognitive Domain in the Human Cerebral Cortex. Springer, Wien.
Geyer, S., Ledberg, A., Schleicher, A., Kinomura, S., Schormann, T., Burgel, U., Klingberg, T., Larsson, J., Zilles, K., Roland, P.E., 1996. Two different areas within the primary motor cortex of man. Nature 382, 805–807.
Gitelman, D.R., Penny, W.D., Ashburner, J., Friston, K.J., 2003. Modeling regional and psychophysiologic interactions in fMRI: the importance of hemodynamic deconvolution. NeuroImage 19, 200–207.
Gould III, H.J., Cusick, C.G., Pons, T.P., Kaas, J.H., 1986. The relationship of corpus callosum connections to electrical stimulation maps of motor, supplementary motor, and the frontal eye fields in owl monkeys. J. Comp. Neurol. 247, 297–325.
Goyal, M.S., Hansen, P.J., Blakemore, C.B., 2006. Tactile perception recruits functionally related visual areas in the late-blind. NeuroReport 17, 1381–1384.
Grefkes, C., Nowak, D.A., Eickhoff, S.B., Dafotakis, M., Kust, J., Karbe, H., Fink, G.R., 2007. Cortical connectivity after subcortical stroke assessed with functional magnetic resonance imaging. Ann. Neurol.
Halsband, U., Lange, R.K., 2006. Motor learning in man: a review of functional and clinical studies. J. Physiol. Paris 99, 414–424.
Heim, S., Eickhoff, S.B., Ischebeck, A.K., Friederici, A.D., Stephan, K.E., Amunts, K., in press. Effective connectivity of the left BA 44, BA 45, and inferior temporal gyrus during lexical and phonological decisions identified with DCM. Hum. Brain Mapp. (Electronic publication ahead of print) doi:10.1002/hbm.20512.
Johansen-Berg, H., Rushworth, M.F., Bogdanovic, M.D., Kischka, U., Wimalaratna, S., Matthews, P.M., 2002. The role of ipsilateral premotor cortex in hand movement after stroke. Proc. Natl. Acad. Sci. U. S. A. 99, 14518–14523.
Johnson-Frey, S.H., 2003. What's so special about human tool use? Neuron 39, 201–204.
Kiebel, S., Holmes, A.P., 2003. The general linear model, In: Frackowiak, R.S., Friston, K.J., Frith, C.D., Dolan, R.J., Price, C.J., Ashburner, J., Penny, W.D., Zeki, S. (Eds.), Human Brain Function, 2 ed. Academic Press, pp. 725–760.
Lindberg, P.G., Schmitz, C., Engardt, M., Forssberg, H., Borg, J., 2007. Use-dependent up- and down-regulation of sensorimotor brain circuits in stroke patients. Neurorehabil. Neural Repair 21, 315–326.
Lundborg, G., 2000. Brain plasticity and hand surgery: an overview. J. Hand Surg. [Br.] 25, 242–252.
Malikovic, A., Amunts, K., Schleicher, A., Mohlberg, H., Eickhoff, S.B., Wilms, M., Palomero-Gallagher, N., Armstrong, E., Zilles, K., 2007. Cytoarchitectonic analysis of the human extrastriate cortex in the region of V5/MT+: a probabilistic, stereotaxic map of area hOc5. Cereb. Cortex 17, 562–574.
Maravita, A., Iriki, A., 2004. Tools for the body (schema). Trends Cogn. Sci. 8, 79–86.
Mayston, M.J., Harrison, L.M., Stephens, J.A., 1999. A neurophysiological study of mirror movements in adults and children. Ann. Neurol. 45, 583–594.
Murase, N., Duque, J., Mazzocchio, R., Cohen, L.G., 2004. Influence of interhemispheric interactions on motor function in chronic stroke. Ann. Neurol. 55, 400–409.
Nowak, D.A., Grefkes, C., Dafotakis, M., Kust, J., Karbe, H., Fink, G.R., 2007. Dexterity is impaired at both hands following unilateral subcortical middle cerebral artery stroke. Eur. J. Neurosci. 25, 3173–3184.
Nowak, D.A., Grefkes, C., Dafotakis, M., Eickhoff, S.B., Kust, J., Karbe, H., Fink, G.R., in press. Effects of low-frequency rTMS over contralesional M1 on movement kinematics and neural activity in subcortical stroke. Arch.Neurol.
Nudo, R.J., Wise, B.M., SiFuentes, F., Milliken, G.W., 1996. Neural substrates for the effects of rehabilitative training on motor recovery after ischemic infarct. Science 272, 1791–1794.
Nudo, R.J., Larson, D., Plautz, E.J., Friel, K.M., Barbay, S., Frost, S.B., 2003. A squirrel monkey model of poststroke motor recovery. ILAR J. 44, 161–174.
Oldfield, R.C., 1971. The assessment and analysis of handedness: the Edinburgh inventory. Neuropsychologia 9, 97–113.
Piza-Katzer, H., Bauer, T., Biedermann, R., Estermann, D., 2006. [Heterotopic hand replantation following radical tumor resection in the elbow region. Functional results 15 months after surgery]. Orthopade 35, 791–797.
Pizzi, M., Brunelli, G., Barlati, S., Spano, P., 2006. Glutamatergic innervation of rat skeletal muscle by supraspinal neurons: a new paradigm in spinal cord injury repair. Curr. Opin. Neurobiol. 16, 323–328.
Rizzolatti, G., Luppino, G., 2001. The cortical motor system. Neuron 31, 889–901.
Rizzolatti, G., Fogassi, L., Gallese, V., 2002. Motor and cognitive functions of the ventral premotor cortex. Curr. Opin. Neurobiol. 12, 149–154.
Rottschy, C., Eickhoff, S.B., Schleicher, A., Mohlberg, H., Kujovic, M., Zilles, K., Amunts, K., 2007. The ventral visual cortex in humans: cytoarchitectonic mapping of two extrastriate areas. Hum. Brain Mapp. 28 (10), 1045–1059.
Rouiller, E.M., Babalian, A., Kazennikov, O., Moret, V., Yu, X.H., Wiesendanger, M., 1994. Transcallosal connections of the distal forelimb representations of the primary and supplementary motor cortical areas in macaque monkeys. Exp. Brain Res. 102, 227–243.

Please cite this article as: Eickhoff, S.B., et al., Central adaptation following heterotopic hand replantation probed by fMRI and effective connectivity analysis, Exp. Neurol. (2008), doi:10.1016/j.expneurol.2008.03.025

Saur, D., Lange, R., Baumgaertner, A., Schraknepper, V., Willmes, K., Rijntjes, M., Weiller, C., 2006. Dynamics of language reorganization after stroke. Brain 129, 1371–1384.

Schaechter, J.D., Moore, C.I., Connell, B.D., Rosen, B.R., Dijkhuizen, R.M., 2006. Structural and functional plasticity in the somatosensory cortex of chronic stroke patients. Brain 129, 2722–2733.

Schallert, T., Leasure, J.L., Kolb, B., 2000. Experience-associated structural events, subependymal cellular proliferative activity, and functional recovery after injury to the central nervous system. J. Cereb. Blood Flow Metab. 20, 1513–1528.

Schallert, T., Woodlee, M.T., Fleming, S.M., 2003. Experimental focal ischemic injury: behavior–brain interactions and issues of animal handling and housing. ILAR J. 44, 130–143.

Stephan, K.E., Harrison, L.M., Penny, W.D., Friston, K.J., 2004. Biophysical models of fMRI responses. Curr. Opin. Neurobiol. 14, 629–635.

Takeuchi, N., Chuma, T., Matsuo, Y., Watanabe, I., Ikoma, K., 2005. Repetitive transcranial magnetic stimulation of contralesional primary motor cortex improves hand function after stroke. Stroke 36, 2681–2686.

Taniwaki, T., Okayama, A., Yoshiura, T., Togao, O., Nakamura, Y., Yamasaki, T., Ogata, K., Shigeto, H., Ohyagi, Y., Kira, J., Tobimatsu, S., 2006. Functional network of the basal ganglia and cerebellar motor loops in vivo: different activation patterns between self-initiated and externally triggered movements. NeuroImage 31, 745–753.

Vogt, S., Buccino, G., Wohlschlager, A.M., Canessa, N., Shah, N.J., Zilles, K., Eickhoff, S.B., Freund, H.J., Rizzolatti, G., Fink, G.R., 2007. Prefrontal involvement in imitation learning of hand actions: effects of practice and expertise. NeuroImage 37, 1371–1383.

Ward, N.S., Cohen, L.G., 2004. Mechanisms underlying recovery of motor function after stroke. Arch. Neurol. 61, 1844–1848.

Wassermann, E.M., Fuhr, P., Cohen, L.G., Hallett, M., 1991. Effects of transcranial magnetic stimulation on ipsilateral muscles. Neurology 41, 1795–1799.

Weiller, C., Chollet, F., Friston, K.J., Wise, R.J., Frackowiak, R.S., 1992. Functional reorganization of the brain in recovery from striatocapsular infarction in man. Ann. Neurol. 31, 463–472.

Wilms, M., Eickhoff, S.B., Specht, K., Amunts, K., Shah, N.J., Malikovic, A., Fink, G.R., 2005. Human V5/MT+: comparison of functional and cytoarchitectonic data. Anat. Embryol.(Berl.) 210, 485–495.

Windhager, R., Millesi, H., Kotz, R., 1995. Resection–replantation for primary malignant tumours of the arm. An alternative to fore-quarter amputation. J. Bone Jt. Surg., Br. vol. 77, 176–184.

Please cite this article as: Eickhoff, S.B., et al., Central adaptation following heterotopic hand replantation probed by fMRI and effective connectivity analysis, Exp. Neurol. (2008), doi:10.1016/j.expneurol.2008.03.025